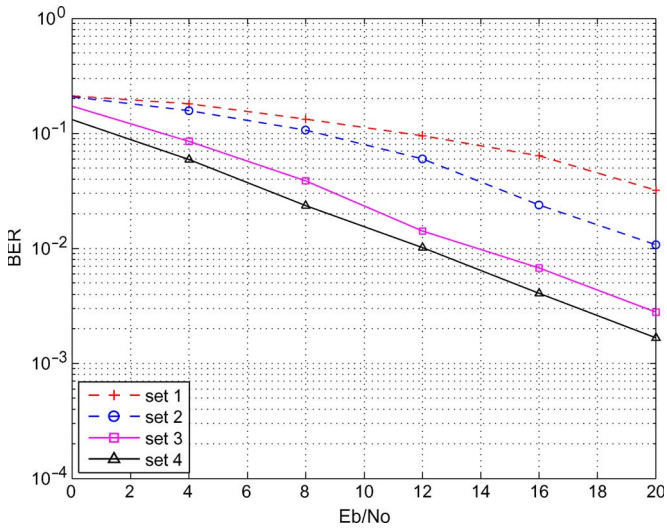

Fig. 5. Effect of the pilot placement with $M = 2$ (200-Hz Doppler frequency).

REFERENCES

[1] K. W. Park and Y. S. Cho, "An MIMO–OFDM technique for high-speed mobile channels," *IEEE Commun. Lett.*, vol. 9, no. 7, pp. 604–606, Jul. 2005.

[2] Y. Zhang and H. Liu, "Frequency-domain correlative coding for MIMO–OFDM systems over fast fading channels," *IEEE Commun. Lett.*, vol. 10, no. 5, pp. 347–349, May 2006.

[3] Y. Li, "Pilot-symbol-aided channel estimation for OFDM in wireless systems," *IEEE Trans. Veh. Technol.*, vol. 49, no. 4, pp. 1207–1215, Jul. 2000.

[4] D. K. Borah and B. D. Hart, "Frequency-selective fading channel estimation with a polynomial time-varying channel model," *IEEE Trans. Commun.*, vol. 47, no. 6, pp. 862–873, Jun. 1999.

[5] W. C. Jakes, *Microwave Mobile Communications*. New York: Wiley, 1974.

[6] J. Du and Y. Li, "MIMO–OFDM channel estimation based on subspace tracking," in *Proc. IEEE VTC*, 2003, pp. 1084–1088.

[7] Y. Li, "Simplified channel estimation for OFDM systems with multiple transmit antennas," *IEEE Trans. Wireless Commun.*, vol. 1, no. 1, pp. 67–75, Jan. 2002.

[8] S. Coleri, M. Ergen, A. Puri, and A. Bahai, "Channel estimation techniques based on pilot arrangement in OFDM systems," *IEEE Trans. Broadcast.*, vol. 48, no. 3, pp. 223–229, Sep. 2002.

[9] J. Gao and H. Liu, "Decision-directed estimation of MIMO time-varying Rayleigh fading channels," *IEEE Trans. Wireless Commun.*, vol. 4, no. 4, pp. 1412–1417, Jul. 2005.

[10] A. Leon-Garcia, *Probability and Random Processes for Electrical Engineering*. Reading, MA: Addison-Wesley, 1993.

[11] D. A. Gore, R. W. Heath, Jr., and A. J. Paulraj, "Transmit selection in spatial multiplexing systems," *IEEE Commun. Lett.*, vol. 6, no. 11, pp. 491–493, Nov. 2002.

[12] J. Li and M. Kavehrad, "Effects of time selective multipath fading on OFDM systems for broadband mobile applications," *IEEE Commun. Lett.*, vol. 3, no. 12, pp. 332–334, Dec. 1999.

[13] G. L. Stuber, J. R. Barry, S. W. Mclaughlin, Y. Li, M. A. Ingram, and T. G. Pratt, "Broadband MIMO–OFDM wireless communications," *Proc. IEEE*, vol. 92, no. 2, pp. 271–294, Feb. 2004.

[14] Y. Zhang and H. Liu, "Impact of time-selective fading on the performance of quasi-orthogonal space–time coded OFDM systems," *IEEE Trans. Commun.*, vol. 54, no. 2, pp. 251–260, Feb. 2006.

[15] Y. Li, L. J. Cimini, and N. R. Sollenberger, "Robust channel estimation for OFDM systems with rapid dispersive fading channels," *IEEE Trans. Commun.*, vol. 46, no. 7, pp. 902–915, Jul. 1998.

[16] A. Stamoulis, S. N. Diggavi, and N. Al-Dhahir, "Intercarrier interference in MIMO OFDM," *IEEE Trans. Signal Process.*, vol. 50, no. 10, pp. 2451–2464, Oct. 2002.

[17] S. Chen and T. Yao, "Intercarrier interference suppression and channel estimation for OFDM systems in time-varying frequency-selective fading channels," *IEEE Trans. Consum. Electron.*, vol. 50, no. 2, pp. 429–435, May 2004.

On the Transmitter-Based Preprocessing for 2-D OFDM-CDMA Forward-Link Systems Over Time-Varying Rayleigh Fading Channels

Chih-Cheng Kuo, *Student Member, IEEE*, Wern-Ho Sheen, *Member, IEEE*, Chung-Ju Chang, *Fellow, IEEE*, and Chang Lung Hsiao, *Member, IEEE*

***Abstract*—Transmitter-based preprocessing is investigated for 2-D orthogonal frequency-division multiplexing code-division multiple-access (OFDM-CDMA) forward-link systems for improving performance and shifting signal processing complexity from a mobile unit to a base station. Preprocessing schemes that are based on zero forcing (ZF) with power normalization, minimum mean square error (MMSE), and ZF with multiuser water filling (ZF-MWF) criteria are jointly investigated with 2-D spreading pattern optimization and multiuser scheduling from an information-theoretic viewpoint. Numerical results show that 1) the performance of preprocessing is quite sensitive to the 2-D spreading pattern for SNRs of interest, for example, 20% degradation on the sum data rate is observed for MMSE preprocessing if the spreading pattern is not properly selected; 2) ZF-MWF may substantially outperform the other two criteria depending on the SNRs; and 3) multiuser scheduling provides a significant performance improvement on the system sum data rate.**

***Index Terms*—Forward-link systems, sum data rate, transmitter preprocessing, two-dimensional (2-D) orthogonal frequency-division multiplexing code-division multiple access (OFDM-CDMA).**

I. INTRODUCTION

Orthogonal frequency-division multiplexing code-division multiple access (OFDM-CDMA) is a promising radio access technology for the next-generation mobile communication systems thanks to its ability to overcome intersymbol interference that is incurred in high-data-rate transmission, its ability to provide universal frequency reuse in a multicell environment, and its ability to achieve high-order diversity gain by spreading data over frequency and time domains [1]–[5]. Traditionally, OFDM and CDMA are combined in a 1-D fashion, that is, a data symbol is spread either in frequency or time domain (see [1] and references therein). Recently, 2-D OFDM-CDMA, where data are spread over time and frequency domains, has been proposed to improve the performance of the 1-D one by simultaneously exploiting the temporal and spectral characteristics of the fading channels [2]–[5].

Transmitter-based preprocessing, on the other hand, has been proposed for improving performance and shifting signal processing complexity from a mobile unit to a base station in mobile communication systems [6]–[13]. Zero forcing (ZF) [6], [7] and prerake [8], [9] preprocessing methods with a different degree of receiver complexity were proposed for direct-sequence CDMA (DS-CDMA) systems. In addition, transmitter preprocessing schemes that are based on the MMSE [11], [13] or ZF [10]–[12] were investigated for broadcast multiple-input–multiple-output (MIMO) systems.

This paper aims to design 2-D OFDM-CDMA forward-link systems with transmitter preprocessing to improve system performance. Three preprocessing methods, including ZF with power normalization (ZF-PN), the MMSE, and ZF with multiuser water filling (ZF-MWF),

Manuscript received August 7, 2006; revised June 11, 2007, July 10, 2007, and August 13, 2007. The review of this paper was coordinated by Prof. J. Choi.

The authors are with the Department of Communication Engineering, National Chiao Tung University, Hsinchu 300, Taiwan, R.O.C. (e-mail: cckuo.cm90g@nctu.edu.tw; whsheen@cm.nctu.edu.tw; cjchang@cc.nctu.edu.tw; clhsiao@itri.org.tw).

Color versions of one or more of the figures in this paper are available online at http://ieeexplore.ieee.org.

Digital Object Identifier 10.1109/TVT.2007.909256

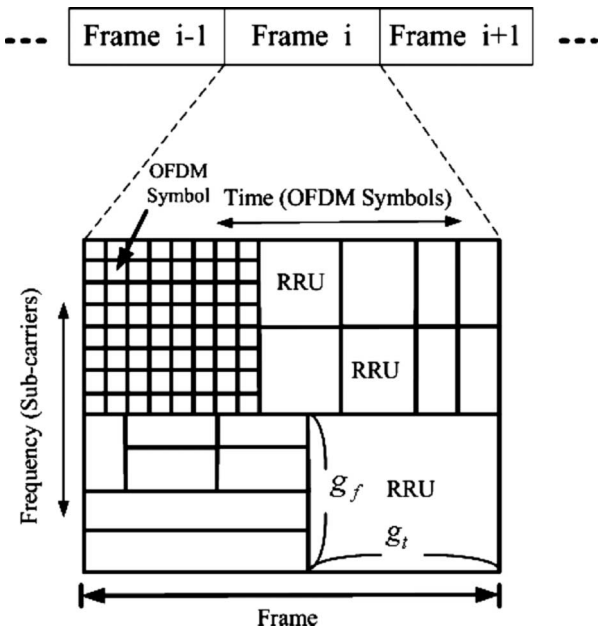

Fig. 1. RRUs.

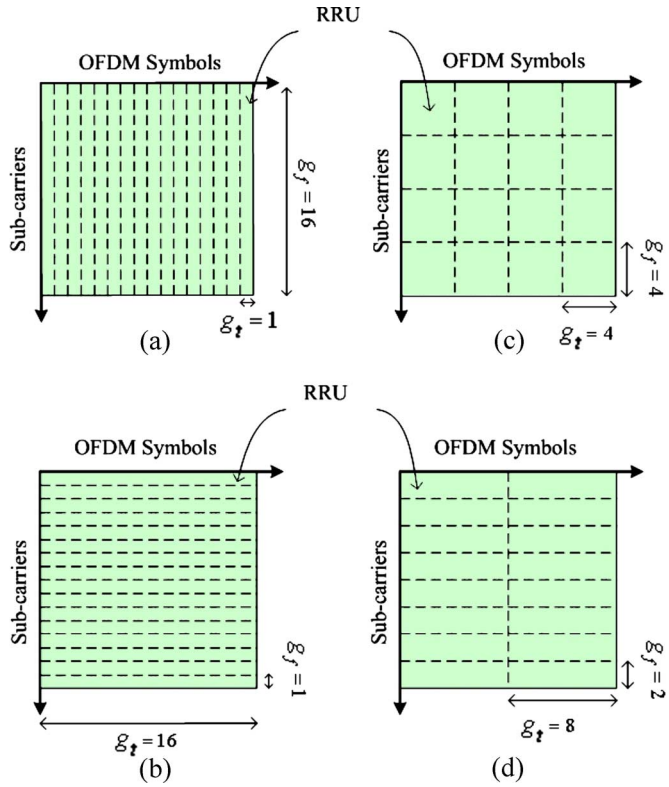

Fig. 2. Example of spreading patterns.

are jointly investigated with spreading pattern optimization and multiuser scheduling from an information-theoretic viewpoint. An ergodic sum data rate serves as the performance index for performance comparisons under the assumption of perfect channel state information (CSI). Numerical results are given to illustrate the superiority of ZF-MWF over the other two methods, the key role that the spreading pattern plays to the system sum data rate, and the performance gain that is obtained through multiuser scheduling.

The rest of this paper is organized as follows. Section II describes the system model. Section III derives the considered transmitter preprocessing methods. Section IV gives the numerical results, and finally, conclusions are given in Section V.

II. System Model

A. RRUs

To apply 2-D spreading, the time–frequency radio resource in a data frame is divided into nonoverlapped $g_f \times g_t$ rectangular radio resource units (RRUs), as shown in Fig. 1, where g_f and g_t are the frequency- and time-domain spreading factors, respectively. $G \coloneqq g_f \times g_t > 1$ is the overall spreading factor. In an RRU, subcarriers and OFDM symbols are assumed to be adjacent to each other. Users with the same overall spreading factor can share an RRU in a code-division fashion, and users with different overall spreading factors utilize different RRUs. Since RRUs are nonoverlapped, without loss of generality, only one RRU will be explicitly treated in the rest of this paper. Note that for $g_t = 1$, the system degenerates to the multicarrier CDMA (MC-CDMA) system, and for $g_f = 1$, the system degenerates to the multicarrier DS-CDMA (MC-DS-CDMA) system that is described in [1]; MC-CDMA and MC-DS-CDMA are special cases of the considered 2-D OFDM-CDMA system.

Different spreading patterns, which are characterized by the pair (g_f, g_t), can be employed for a particular G. Fig. 2 depicts such possibilities for $G = 16$ with different selections of g_f and g_t. For example, $(g_f = 2, g_t = 8)$ and $(g_f = 4, g_t = 4)$ are two legitimate spreading patterns. Different spreading patterns result in different performance, depending on the frequency and time selectivity of the channel, as will be shown in Section IV. In fact, how the spreading patterns perform against each other for a fixed G is one of the issues that interest us in this paper.

Let G also denote the number of users sharing an RRU. (Recall that G is the overall spreading factor.) In a data frame, with orthogonal spreading codes, an RRU can be simultaneously shared by all the G users in a code-division fashion, i.e., one code for each user (the single-code case), or the RRU can be shared by the G users in a time-division fashion, i.e., some users are scheduled to transmit in a frame, and others are scheduled in other frames. In a time-varying fading environment, by scheduling those users who are in a good channel condition in a particular frame, one can take advantage of multiuser diversity to increase the system throughput [11]. In this paper, to investigate the multiuser diversity gain, we allow $K \leqq G$ users to be scheduled in a frame. For that case, each scheduled user utilizes G/K spreading codes (the multicode case) for data transmission, where G/K is a positive integer.

B. Channel Model

A discrete-time wide-sense stationary uncorrelated scattering Rayleigh channel is considered. The complex equivalent low-pass response for the ith user is given by

$$h^{(i)}(t;\tau) = \sum_{l=0}^{L} h_l^{(i)}(t)\delta(\tau - lT_s), \quad i = 1, \ldots, K \tag{1}$$

where $h_l^{(i)}(t)$ is the lth path gain, $\delta(\cdot)$ is the Dirac delta function, lT_s is the propagation delay for the lth path, T_s is the sampling duration of the system, and K is the number of scheduled users. $h_l^{(i)}(t)$ is a complex Gaussian variable with zero mean and variance σ_l^2, $\{h_l^{(i)}(t)\}_{l=0}^{L}$ are independent for different l's, and users experience independent identically distributed (i.i.d.) channel characteristics.

The channel is assumed to remain constant over an OFDM symbol and to vary symbol-by-symbol based on the channel time variation.

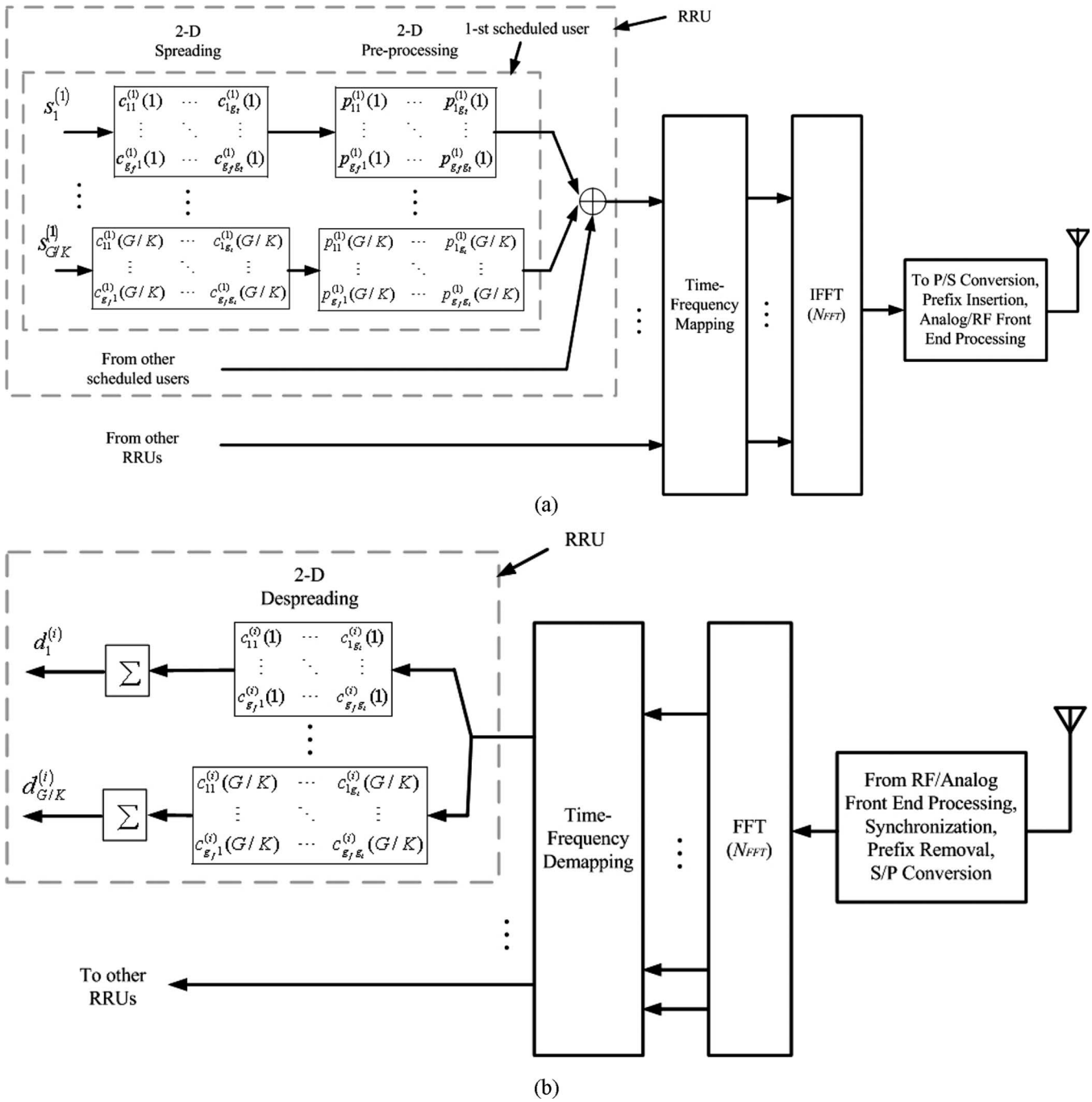

Fig. 3. (a) Transmitter. (b) Receiver.

Thus, (1) can be simplified as

$$h^{(i)}(n;\tau) = \sum_{l=0}^{L} h_l^{(i)}(n)\delta(\tau - lT_s), \quad i = 1, \ldots, K \tag{2}$$

where n is the OFDM symbol index. Furthermore, the power delay profile of the multipath channel follows the exponential decay model

$$\sigma_l^2 = \sigma_0^2 \cdot \exp(-10l/L), \quad l = 1, 2, \ldots, L \tag{3}$$

with $\sigma_0^2 = 1 - \exp(-10/L)$, and it leads to the unit of total power. Last, the Clarke 2-D isotropic scattering model for $\{h_l^{(i)}(n)\}$ will be used to model the time variation of channels in this paper [14].

C. Transmitter and Receiver

The transmitter of the considered OFDM-CDMA forward-link system is sketched in Fig. 3(a). Recall that only one RRU will be explicitly treated. The lth data symbol of user i, i.e., $s_l^{(i)}$, $i = 1, \ldots, K$, $l = 1, \ldots, G/K$ is first spread over time and frequency domains by a 2-D spreading code $c_{m,n}^{(i)}(l)$, $m = 1, \ldots, g_f$, $n = 1, \ldots, g_t$, and the spreading *chip* is preprocessed by multiplying the complex-valued gain $p_{m,n}^{(i)}(l)$. The respective *chips* from all data symbols in an RRU are summed together before being allocated to the time–frequency plane, which is done, along with chips from other RRUs, by time–frequency mapping. Last, the inverse fast Fourier transform (IFFT) is performed on the allocated chips, and these chips are sent for further operations such as parallel-to-serial

conversion, cyclic-prefix insertion, and analog/RF front-end processing.

As shown in Fig. 3(b), at the receive end of the ith user, after RF/analog processing, synchronization, cyclic-prefix removal, and serial-to-parallel conversion, the fast Fourier transform (FFT) and time–frequency demapping are performed on the received signal. The demapped chips of the considered RRU are passed through simple 2-D despreading because most of the signal processing has been shifted to the base station. The despread signals are then forwarded for further demodulation and/or decoding.

D. Signal Models

For notational simplicity, only the single-code case, i.e., $K = G$, one spreading code for each user, is explicitly treated in this section. The extension to the case of multicodes is straightforward. Assuming that the cyclic prefix is larger than the maximum delay spread, and perfect frequency/time synchronization is achieved at the receiver, then the demapped signal of the (m, n)th chip of the ith user is given by

$$r_{m,n}^{(i)}(1) = \left(\sum_{j=1}^{G} s_1^{(j)} p_{m,n}^{(j)}(1) c_{m,n}^{(j)}(1) \right) H_{m,n}^{(i)} + N_{m,n}^{(i)} \quad m = 1, \ldots, g_f,\ n = 1, \ldots, g_t,\ i = 1, \ldots, G \tag{4}$$

where

$$H_{m,n}^{(i)} = \sum_{l=0}^{L} h_l^{(i)}(n) e^{\frac{-j2\pi lm}{N_{\mathrm{FFT}}}} \tag{5}$$

is the frequency-domain channel gain, N_{FFT} is the size of IFFT/FFT, and $N_{m,n}^{(i)}$ is a Gaussian variable with zero mean and variance σ_N^2.

For convenience, we rearrange the 2-D chip index (m, n) into the 1-D one by using $k = (n-1)g_f + m, n = 1, \ldots, g_t, m = 1, \ldots, g_f$, and it leads to $k = 1, \ldots, G$. With this new indexing notation and (4), $\mathbf{r}_1^{(i)}$ can be rewritten as the following matrix form:

$$\begin{aligned} \mathbf{r}_1^{(i)} &\doteq \left[r_1^{(i)}(1), \cdots, r_k^{(i)}(1), \cdots, r_G^{(i)}(1) \right]^T \\ &= \mathbf{H}^{(i)}(\mathbf{P} \odot \mathbf{C})\mathbf{s} + \mathbf{n}^{(i)} \end{aligned} \tag{6}$$

where $\mathbf{P} = [\mathbf{p}^{(1)}, \ldots, \mathbf{p}^{(G)}]$, $\mathbf{p}^{(j)} = [p_1^{(j)}(1), \ldots, p_G^{(j)}(1)]^T$, $\mathbf{s} = [s_1^{(1)}, \ldots, s_1^{(G)}]^T$, $\mathbf{n}^{(i)} = [N_1^{(i)}, \ldots, N_G^{(i)}]^T$, $\mathbf{C} = [\mathbf{c}^{(1)}, \ldots, \mathbf{c}^{(G)}]$, $\mathbf{c}^{(j)} = [c_1^{(j)}(1), \ldots, c_G^{(j)}(1)]^T$, and $\mathbf{H}^{(i)}$ is a diagonal matrix with elements $\{H_1^{(i)}, \ldots, H_G^{(i)}\}$. $\odot$ and $[\cdot]^T$ denote the Hadamard product (element-by-element multiplication) and the operation of transpose of a vector and/or a matrix, respectively, $\mathbf{s}$ is the symbol vector with the covariance matrix $\sigma_s^2 \mathbf{I}_G$, $\mathbf{n}^{(i)}$ is a complex Gaussian vector with the covariance matrix $\sigma_N^2 \mathbf{I}_G$, σ_s^2 is the transmit signal power, σ_N^2 is the noise power for each chip, and $\mathbf{I}_G$ is the identity matrix of dimension G.

Let $d_1^{(i)}$ be the decision variable of the ith user. Then

$$d_1^{(i)} \doteq \mathbf{c}^{(i)^H} \mathbf{r}_1^{(i)} = \mathbf{c}^{(i)^H} \mathbf{H}^{(i)} (\mathbf{P} \odot \mathbf{C})\mathbf{s} + \mathbf{c}^{(i)^H} \mathbf{n}^{(i)} \tag{7}$$

where $[\cdot]^H$ is the conjugate transpose operation, and $\{\mathbf{c}^{(i)^H} \mathbf{n}^{(i)}\}_{i=1}^{G}$ are i.i.d. Gaussian variables, provided that orthogonal codes are used.

III. Transmitter Preprocessing

For a multiple-access system, the sum data rate is the maximum data rate of all users supported by the system from an information-theoretic viewpoint [11, ch. 6 and 8]. The sum data rate will be adopted here as the performance index for the design and the comparison of different preprocessing methods.

From (7), the decision variable for the ith user can be rewritten as

$$\begin{aligned} d_1^{(i)} = & \underbrace{\mathbf{c}^{(i)^H} \mathbf{H}^{(i)} \left(\mathbf{p}^{(i)} \odot \mathbf{c}^{(i)} \right) s_1^{(i)}}_{\text{desired signal}} \\ & + \underbrace{\sum_{j=1, j \neq i}^{G} \mathbf{c}^{(i)^H} \mathbf{H}^{(i)} \left(\mathbf{p}^{(j)} \odot \mathbf{c}^{(j)} \right) s_1^{(j)}}_{\text{MAI}} \\ & + \underbrace{\mathbf{c}^{(i)^H} \mathbf{n}^{(i)}}_{\text{noise}}. \end{aligned} \tag{8}$$

The multiple-access interference (MAI) term can be approximated as a zero-mean Gaussian variable under the assumption of large G [11]. Therefore, the achievable maximum reliable data rate $C^{(i)}$ for the ith user, given $\mathbf{H}^{(i)}$, is presented by (9), shown at the bottom of the page [11], where $\mathbf{q}^{(i)} = \mathbf{p}^{(i)} \odot \mathbf{c}^{(i)}$, and $\|\mathbf{c}^{(i)}\|^2 = 1$ for $i = 1, 2, \ldots, G$. As a result, the sum data rate C, which is the sum of the individual rates, is obtained by (10), shown at the bottom of the page.

With the performance index in (10), our problem becomes finding the set of optimum preprocessing weight vectors $\{\widehat{\mathbf{q}}^{(i)}\}$, for a given

$$C^{(i)} = \frac{1}{G} \log_2 \left\{ 1 + \frac{E\left[\left| \mathbf{c}^{(i)^H} \mathbf{H}^{(i)} q^{(i)} s_1^{(i)} \right|^2 \right]}{E\left[\left| \sum_{j=1, j \neq i}^{G} \mathbf{c}^{(i)^H} \mathbf{H}^{(i)} \mathbf{q}^{(j)} s_1^{(j)} + \mathbf{c}^{(i)^H} \mathbf{n}^{(i)} \right|^2 \right]} \right\} \text{ b/s/Hz} \tag{9}$$

$$C = \sum_{i=1}^{G} C^{(i)} = \frac{1}{G} \sum_{i=1}^{G} \log_2 \left\{ 1 + \frac{\sigma_s^2 \cdot \mathbf{q}^{(i)^H} \mathbf{H}^{(i)^H} \mathbf{c}^{(i)} \mathbf{c}^{(i)^H} \mathbf{H}^{(i)} \mathbf{q}^{(i)}}{\sigma_s^2 \sum\limits_{j=1, j \neq i}^{G} \mathbf{q}^{(j)^H} \mathbf{H}^{(i)^H} \mathbf{c}^{(i)} \mathbf{c}^{(i)^H} \mathbf{H}^{(i)} \mathbf{q}^{(j)} + \sigma_N^2} \right\} \tag{10}$$

$\{\mathbf{H}^{(i)}\}$, to obtain the maximum sum data rate by solving the following constrained optimization problem:

$$\{\widehat{\mathbf{q}}^{(i)}\} = \arg\left\{\max_{\{\mathbf{q}^{(i)}\}} C\right\}, \quad \text{s.t.} \sum_{i=1}^{G} \left\|\mathbf{q}^{(i)}\right\|^2 = G. \tag{11}$$

After obtaining the sum data rate for a particular $\{\mathbf{H}^{(i)}\}$, the average sum data rate, called the ergodic sum data rate in [11, ch. 6 and 8], is evaluated by $C_{\text{erg}} = E[C]$, where the expectation is taken over all channels $\{\mathbf{H}^{(i)}\}$.

The following investigates three transmitter preprocessing methods based on ZF-PN, MMSE, and ZF-MWF criteria under the perfect knowledge of CSI of every user. Since the optimization formulation in (10) and (11) is similar to the one investigated in [11] and [12] for MIMO systems, only sketches of the derivations are given here.

A. ZF-PN

The basic idea of this method is to completely eliminate the MAI at the outputs of despreading of each user by properly choosing the transmitter preprocessing matrix $\mathbf{Q} = \mathbf{P} \odot \mathbf{C}$ at the base station under the power constraint given in (11).

Define $\mathbf{d}$ to be the aggregated decision variables from all users. From (7)

$$\begin{aligned}\mathbf{d} &\doteq \begin{bmatrix} d_1^{(1)} \\ \vdots \\ d_1^{(G)} \end{bmatrix} = \begin{bmatrix} \mathbf{c}^{(1)H} & \mathbf{H}^{(1)}\mathbf{Q}\mathbf{s} + \mathbf{c}^{(1)H} & \mathbf{n}^{(1)} \\ & \vdots & \\ \mathbf{c}^{(G)H} & \mathbf{H}^{(G)}\mathbf{Q}\mathbf{s} + \mathbf{c}^{(G)H} & \mathbf{n}^{(G)} \end{bmatrix} \\ &= \begin{bmatrix} \mathbf{c}^{(1)H} & \mathbf{H}^{(1)} \\ \vdots & \\ \mathbf{c}^{(G)H} & \mathbf{H}^{(G)} \end{bmatrix} \mathbf{Q}\mathbf{s} + \begin{bmatrix} \mathbf{c}^{(1)H} & \mathbf{n}^{(1)} \\ \vdots & \\ \mathbf{c}^{(G)H} & \mathbf{n}^{(G)} \end{bmatrix} \\ &= \underbrace{\mathbf{R}\mathbf{Q}\mathbf{s}}_{\text{signal}} + \underbrace{\mathbf{n}}_{\text{noise}}\end{aligned} \tag{12}$$

where

$$\mathbf{R} = \begin{bmatrix} \mathbf{c}^{(1)H} & \mathbf{H}^{(1)} \\ \vdots & \\ \mathbf{c}^{(G)H} & \mathbf{H}^{(G)} \end{bmatrix}$$

$$\mathbf{n} = \begin{bmatrix} \mathbf{c}^{(1)H} & \mathbf{n}^{(1)} \\ \vdots & \\ \mathbf{c}^{(G)H} & \mathbf{n}^{(G)} \end{bmatrix}.$$

With zero MAI, $\mathbf{R}\widetilde{\mathbf{Q}}\mathbf{s} = \mathbf{s}$, which results in

$$\widetilde{\mathbf{Q}} = \mathbf{R}^H(\mathbf{R}\mathbf{R}^H)^{-1} \doteq \mathbf{R}^+ \tag{13}$$

where $\mathbf{R}^+$ is the right pseudoinverse of matrix $\mathbf{R}$. On the other hand, according to (11), the total transmit power needs to be normalized to $\sigma_s^2 G$, that is, $E[\|\widehat{Q}s\|^2] = \sigma_s^2 \cdot G$. Therefore, $\widehat{\mathbf{Q}} = \sqrt{G}\mathbf{R}^+/\|\mathbf{R}^+\|_F$ [6], where $\|\cdot\|_F$ stands for the Frobenius norm of a matrix.

B. MMSE

In this method, $\widehat{\mathbf{Q}}$ is selected to minimize the MSE between the decision vector $\mathbf{d}$ and the transmitted symbol vector $\mathbf{s}$ under fixed transmit power. The associated constrained optimization problem can be formulated as follows:

$$\widehat{\mathbf{Q}} = \arg\left\{\min_{\mathbf{Q}} E\left[\|\mathbf{d}-\mathbf{s}\|^2\right]\right\}, \quad \text{s.t.} \|\mathbf{Q}\|_F^2 = \text{tr}\{\mathbf{Q}^H\mathbf{Q}\} = G \tag{14}$$

where

$$\begin{aligned}E\left[\|\mathbf{d}-\mathbf{s}\|^2\right] &= E\left[\|\mathbf{R}\mathbf{Q}\mathbf{s}+\mathbf{n}-\mathbf{s}\|^2\right] \\ &= \sigma_s^2 \text{tr}\left\{\left[\mathbf{Q}^H\mathbf{R}^H - \mathbf{I}_G\right][\mathbf{R}\mathbf{Q} - \mathbf{I}_G]\right\} + G\sigma_N^2.\end{aligned} \tag{15}$$

Therefore, (14) can be rewritten as

$$\widehat{\mathbf{Q}} = \arg\left\{\min_{\mathbf{Q}} \text{tr}\left\{\left[\mathbf{Q}^H\mathbf{R}^H - \mathbf{I}_G\right][\mathbf{R}\mathbf{Q} - \mathbf{I}_G]\right\}\right\} \quad \text{s.t.} \|\mathbf{Q}\|_F^2 = \text{tr}\{\mathbf{Q}^H\mathbf{Q}\} = G. \tag{16}$$

By applying the theory of Lagrange multiplier to solve the above constrained optimization problem, the solution is [13]

$$\widehat{\mathbf{Q}} = (\mathbf{R}^H\mathbf{R} + \widehat{\lambda} \cdot \mathbf{I}_G)^{-1}\mathbf{R}^H \tag{17}$$

and $\widehat{\lambda}$ satisfies $\sum_{i=1}^{G}(\lambda_i/(\widehat{\lambda}+\lambda_i)^2) = G$, where $\{\lambda_i\}$ are the eigenvalues of the matrix $\mathbf{R}^H\mathbf{R}$.

C. ZF-MWF

In this method, multiuser water filling is exploited to improve the performance of ZF-PN. This is done in two steps. First, the desired signal power for each user is maximized under the condition of zero MAI. It is equivalent to finding a set of $\{\widetilde{\mathbf{q}}^{(i)}\}$ such that

$$\widetilde{\mathbf{q}}^{(i)} = \arg\left\{\max_{\mathbf{q}^{(i)}} \mathbf{q}^{(i)H}\mathbf{H}^{(i)H}\mathbf{c}^{(i)}\mathbf{c}^{(i)H}\mathbf{H}^{(i)}\mathbf{q}^{(i)}\right\} \quad \text{s.t.} \ \mathbf{q}^{(i)} \in \bigcap_{j=1, j\neq i}^{G} N\left\{\mathbf{H}^{(j)H}\mathbf{c}^{(j)}\mathbf{c}^{(j)H}\mathbf{H}^{(j)}\right\} \forall I \tag{18}$$

where $N\{\mathbf{A}\}$ denotes the null space of the matrix $\mathbf{A}$, and $\cap$ is the operation of intersection. Using $\{\widetilde{\mathbf{q}}^{(i)}\}$ obtained in (18), the sum data rate in (10) becomes

$$C = \frac{1}{G}\sum_{i=1}^{G} \log_2\left\{1 + \frac{\sigma_s^2\alpha^{(i)}\left\|\widetilde{\mathbf{q}}^{(i)}\right\|^2}{\sigma_N^2}\right\} \tag{19}$$

where $\alpha^{(i)}$ is a function of $\{\mathbf{H}^{(i)}\}$ and can be viewed as the equivalent channel power gain that is experienced by the ith user [11], [12]. Second, the principle of multiuser water filling is applied in (19) to obtain the maximum sum data rate. That is, we are seeking

$$\left\{\left\|\widehat{\mathbf{q}}^{(i)}\right\|^2\right\} = \arg\left\{\max_{\left\{\left\|\widetilde{\mathbf{q}}^{(i)}\right\|^2\right\}} \sum_{i=1}^{G} \log_2\left[1 + \frac{\sigma_s^2\alpha^{(i)}\left\|\widetilde{\mathbf{q}}^{(i)}\right\|^2}{\sigma_N^2}\right]\right\} \quad \text{s.t.} \sum_{i=1}^{G}\left\|\widetilde{\mathbf{q}}^{(i)}\right\|^2 = G. \tag{20}$$

Again, by applying the theory of Lagrange multiplier, it can be shown that

$$\left\|\widehat{\mathbf{q}}^{(i)}\right\|^2 = \left[1 + \frac{1}{G}\sum_{j=1}^{G}\frac{\sigma_N^2}{\sigma_s^2\alpha^{(j)}} - \frac{\sigma_N^2}{\sigma_s^2\alpha^{(i)}}\right]^+ \quad \forall i \tag{21}$$

where $[x]^+ = \max\{x, 0\}$.

TABLE I
SYSTEM PARAMETERS

Parameters	Values
Number of users in the system, G	16
Overall processing gain, G	16
Values of g_t and/or g_f	1, 2, 4, 8, 16
Number of users scheduled in a frame, K	1, 2, 4, 8, 16
Number of spreading codes allocated to each scheduled user	G/K
OFDM symbol duration, T_{OFDM}	10 μs
Useful OFDM symbol duration, T_{FFT}	8 μs
Sub-carrier frequency spacing, $\Delta f = 1/T_{FFT}$	125 KHz
System sampling period, T_s	T_{FFT}/N_{FFT}
FFT size, N_{FFT}	256
Cyclic prefix size	64
Normalized frequency selectivity, $\Delta f/B_c$, B_c: coherent bandwidth of the channel	1/8, 1/4, 1/2
Frame size	64 OFDM symbols
Normalized time selectivity, T_{OFDM}/T_c, T_c: coherent time of the channel	1/8, 1/4, 1/2
Spreading Codes	Hadamard-Walsh codes

IV. NUMERICAL RESULTS

This section presents and compares the ergodic sum data rate of the considered preprocessing methods. The system parameters are summarized in Table I. Recall that there are a total of G users in the system; however, they may not all be scheduled to transmit in a frame. $K \leqq G$ denotes the actual number of scheduled users. For $K < G$, G/K codes are allocated to each user (multicode transmission), and the system can exploit the multiuser diversity gain to increase the sum data rate. The user scheduling is performed on a frame-by-frame basis. As given in Table I, a frame consists of 64 OFDM symbols. The Hadamard–Walsh orthogonal codes are used throughout this paper.

In Table I, $\Delta f/B_c$ and T_{OFDM}/T_c are defined as the normalized frequency and time selectivity, respectively, where B_c is the coherent bandwidth, and T_c is the coherent time of the channel. In this paper, $B_c = 1/(50\sigma_\tau)$, and $T_c = 1/(50 f_D)$, where σ_τ is the root-mean-square delay spread, and f_D is the maximum Doppler spread of the channel [14]. By changing the path number L and f_D, we can obtain the desirable frequency and time selectivity designated in Table I. For example, $L = 7$, 13, and 26 correspond to $\Delta f/B_c = 1/8,\ 1/4,$ and $1/2$, and $f_D = 250,\ 500,$ and 1000 Hz correspond to $T_{\mathrm{OFDM}}/T_c = 1/8,\ 1/4,$ and $1/2$, respectively. The number of channel samples that are used to evaluate the ergodic sum data rate is over 20 000.

Fig. 4 shows an example effect of spreading patterns on the performance of the preprocessing methods for the case of SNR = 29 dB. Similar results are observed for other SNRs. Obviously, the best spread pattern is the one that reduces the channel selectivity in time and frequency domains. In other words, the spread pattern has to be selected to reduce the MAI for better performance. In this example, $g_f = 4$, $g_t = 4$ is the optimum one, regardless of the channel selectivity. The loss in the ergodic sum data rate can be quite large if the spreading pattern is not properly selected; for example, over 20% loss is observed for MMSE preprocessing. Also shown in the figure is that the channel selectivity degrades system capacity; the degradation is the most significant for MMSE preprocessing.

Fig. 5 compares the ergodic sum data rates for different SNRs in selective channels with $K = 16$. Frequency-domain spreading with two values of the channel selectivity, that is, $\Delta f/B_c = 1/4$ and $1/2$, is used as the example. As shown in the figure, the channel selectivity

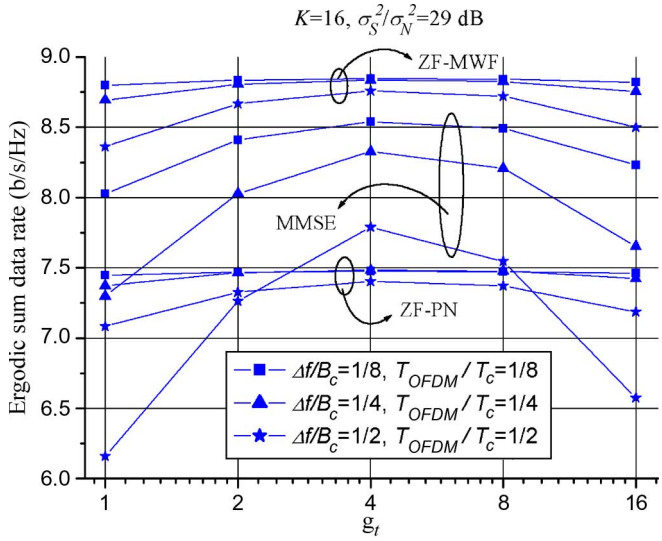

Fig. 4. Example effects of spreading patterns on the ergodic sum data rate with different degrees of selectivity with $\sigma_s^2/\sigma_N^2 = 29$ dB.

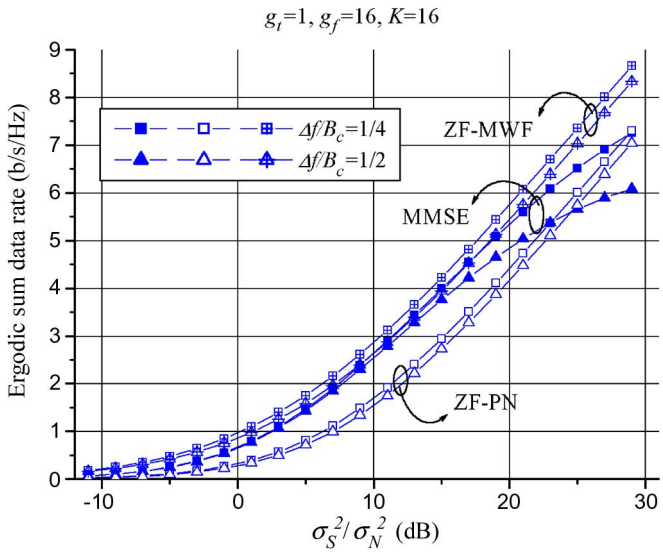

Fig. 5. Comparisons of the ergodic sum data rate for different preprocessing methods with $\Delta f/B_c = 1/4$ and $\Delta f/B_c = 1/2$.

decreases the ergodic sum data rate; the more severe the channel selectivity, the smaller the ergodic sum data rate. This phenomenon is more prominent for the MMSE in the high SNR region because in the MMSE, there is a residual MAI, which becomes more dominant in performance at the high SNR region. The ZF-MWF could significantly outperform the other two criteria, depending on the channel selectivity, and the operating SNR. ZF-PN performs less favorably than the other two criteria in the low SNR region. Nevertheless, it outperforms the MMSE in the high SNR region where the MAI is the dominant factor.

Fig. 6 shows the performance of the ergodic sum data rate for the nonselective channel with a different number of scheduled users. For comparison purposes, the sum data rate for the additive white Gaussian noise (AWGN) channel is also included in the figure. Clearly, for $K \leqq 8$, a higher ergodic sum data rate is obtained for fading channels than that for the AWGN case because of the exploitation of the multiuser diversity. Nevertheless, the advantage of the multiuser diversity diminishes as the number of scheduled users becomes larger.

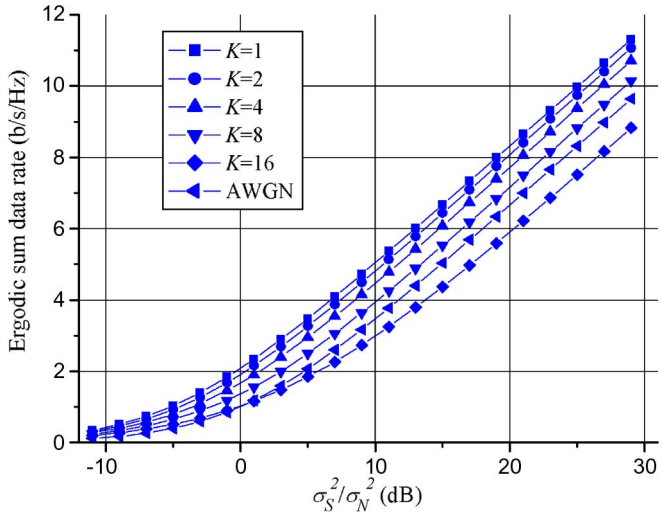

Fig. 6. Ergodic sum data rate of ZF-MWF for nonselective channels with multiuser scheduling.

In fact, for $K = 16$, the ergodic sum data rate of the fading channel is less than that of the AWGN channel, except for very low SNRs.

V. Conclusion

Different transmitter-based preprocessing methods are jointly investigated with spreading pattern optimization and multiuser scheduling for the 2-D OFDM-CDMA forward-link systems from an information-theoretic viewpoint. The ergodic sum data rate serves as the performance index for performance comparisons under the assumption of perfect CSI. Examples are given to illustrate the important issue of spreading pattern optimization. ZF-MWF performs the best among the preprocessing methods that were investigated, including ZF and the MMSE. Moreover, as expected, multiuser scheduling gives a significant performance improvement.

References

[1] S. Hara and R. Prasad, "Overview of multicarrier CDMA," *IEEE Commun. Mag.*, vol. 35, no. 12, pp. 126–133, Dec. 1997.

[2] H. Atarashi, S. Abeta, and M. Sawahashi, "Variable spreading factor orthogonal frequency and code division multiplexing (VSF-OFCDM) for broadband packet wireless access," *IEICE Trans. Commun.*, vol. E86-B, no. 1, pp. 291–299, Jan. 2003.

[3] A. Persson, T. Ottosson, and E. Strom, "Time–frequency localized CDMA for downlink multi-carrier systems," in *Proc. IEEE ISSSTA*, Prague, Czech Republic, Sep. 2002, pp. 118–122.

[4] K. Zheng, G. Zeng, L. Lei, and W. Wang, "Performance analysis for synchronous OFDM-CDMA with joint frequency–time spreading," in *Proc. IEEE ICC*, Paris, France, Jun. 2004, pp. 3304–3308.

[5] W.-H. Sheen and J.-S. Sheu, "On the adaptability of OFDM-CDMA forward link with time–frequency spreading in multi-path fading channels," in *Proc. IEEE VTC—Fall*, Dallas, TX, Sep. 2005, pp. 617–621.

[6] B. R. Vojcic and W. M. Jang, "Transmitter precoding in synchronous multiuser communications," *IEEE Trans. Commun.*, vol. 46, no. 10, pp. 1346–1355, Oct. 1998.

[7] M. B. Pearce and A. Dharap, "Transmitter-based multiuser interference rejection for the down-link of a wireless CDMA systems in a multipath environment," *IEEE J. Sel. Areas Commun.*, vol. 18, no. 3, pp. 407–417, Mar. 2000.

[8] R. L. Choi, K. B. Letaief, and R. D. Murch, "MISO CDMA transmission with simplified receiver for wireless communication handsets," *IEEE Trans. Commun.*, vol. 49, no. 5, pp. 888–898, May 2001.

[9] R. Esmailzadeh, E. Sourour, and M. Nakagawa, "Prerake diversity combining in time division duplex CDMA mobile communications," *IEEE Trans. Veh. Technol.*, vol. 48, no. 3, pp. 795–801, May 1999.

[10] L. Choi and R. D. Murch, "A transmit preprocessing technique for multiuser MIMO systems using a decomposition approach," *IEEE Trans. Wireless Commun.*, vol. 3, no. 1, pp. 20–24, Jan. 2004.

[11] D. Tse and P. Viswanath, *Fundamentals of Wireless Communication*. Cambridge, U.K.: Cambridge Univ. Press, 2005.

[12] T. Yoo and A. Goldsmith, "On the optimality of multiantenna broadcast scheduling using zero-forcing beamforming," *IEEE J. Sel. Areas Commun.*, vol. 24, no. 3, pp. 528–541, Mar. 2006.

[13] J. Liu and A. Duel-Hallen, "Linear multiuser precoding with transmit antenna diversity for DS/CDMA systems," in *Proc. IEEE MILCOM*, Oct. 2005, pp. 2823–2829.

[14] T. S. Rappaport, *Wireless Communication: Principles and Practice*. Upper Saddle River, NJ: Prentice-Hall, 1996.

Interpretation of MIMO Channel Characteristics in Rectangular Tunnels From Modal Theory

J. M. Molina-Garcia-Pardo, *Member, IEEE*, Martine Lienard, Pierre Degauque, *Member, IEEE*, Donald G. Dudley, *Fellow, IEEE*, and L. Juan-Llacer, *Senior Member, IEEE*

***Abstract*—We develop a modal approach for analyzing multiple-input–multiple-output (MIMO) wireless channel propagation in a tunnel with lossy walls. We use parametric methods to study the effects of the number of modes and of the separation among antennas. We evaluate the performance of the MIMO channel in terms of capacity as a function of range and tunnel size.**

***Index Terms*—Modal theory, modes, multiple-input–multiple-output (MIMO), propagation in tunnels, ray tracing.**

I. Introduction

This paper builds on the information-theoretic result that multiple-input–multiple-output (MIMO) channels offer a substantial improvement over a single channel. Specifically, the Foschini–Telatar MIMO model [1], [2] predicts a dramatic increase in channel capacity over the Shannon single-channel capacity [3, Ch. 11]. An overview of MIMO wireless communications is provided in [4] and [5]. In addition, the ideas have been explored in depth in [6]. Our application of MIMO

Manuscript received January 17, 2006; revised January 30, 2007, June 28, 2007, and August 28, 2007. The work of J. M. Molina-Garcia-Pardo at the University of Lille was supported by the Universidad Politecnica de Cartagena. This work was supported in part by Pole Sciences et Technologies pour la Securite dans les Transports (Science and Technology for Safety in Transportation) and in part by the European Commission (FEDER), the French Ministry of Research, and the Region Nord Pas de Calais. The review of this paper was coordinated by Prof. A. Abdi.

J. M. Molina-Garcia-Pardo was with the Telecommunications, Interferences and Electromagnetic Compatibility (TELICE), Institut d'Electronique de Microelectronique et de Nanotechnologie, University of Lille, 59655 Villeneuve d'Ascq, France. He is now with the Departamento de Technologias de la Información y la Comunicaciones, Technical University of Cartagena, 30202 Cartagena, Spain (e-mail: josemariamolina@upct.es).

M. Lienard and P. Degauque are with the Telecommunications, Interferences and Electromagnetic Compatibility (TELICE), Institut d'Electronique de Microelectronique et de Nanotechnologie, University of Lille, 59655 Villeneuve d'Ascq, France (e-mail: Martine.Lienard@univ-lille1.fr).

D. G. Dudley, deceased, was with the Department of Electrical and Computer Engineering, University of Arizona, Tucson, AZ 85721 USA.

L. Juan-Llacer is with the Departamento de Technologias de la Información y la Comunicaciones, Technical University of Cartagena, 30202 Cartagena, Spain.

Digital Object Identifier 10.1109/TVT.2007.913177